ELSEVIER

Polymer 42 (2001) 8517–8527

polymer

www.elsevier.com/locate/polymer

Fibers spun from poly(ethylene terephthalate) blended with a thermotropic liquid crystalline copolyester with non-coplanar biphenylene units

Werner Grasser[1], Hans-Werner Schmidt, Reiner Giesa*

Macromolecular Chemistry I, Bayreuth Institute for Macromolecular Research (BIMF) and Laboratory for Polymer Processing, Universität Bayreuth, D-95440 Bayreuth, Germany

Received 22 April 2001; received in revised form 11 May 2001; accepted 20 May 2001

Abstract

To investigate the potential of a fully aromatic, amorphous thermotropic liquid crystalline polyester (CPHNA60) as the in situ reinforcement component for poly(ethylene terephthalate) (PET) fibers, blends containing up to 10 wt% of CPHNA60 were prepared, characterized and spun into fibers. DSC measurements of the blends revealed a nucleating effect of CPHNA60 and rheology investigations showed a decreased melt viscosity even at 0.5 wt% CPHNA60 content. Blend fibers were spun at temperatures between 270 and 290°C and successively cold and hot drawn. As-spun fibers showed an increase in Young's modulus with increasing CPHNA60 content to 5.8 GPa at 10 wt%. After a two stage drawing process, moduli up to 22.6 GPa at 3 wt% load level were measured while maintaining ultimate strength values around 1 GPa. This correlates to an increase in modulus of 22%. SEM experiments of as-spun fiber fracture surfaces showed uniformly dispersed CPHNA60 fibrils within the PET matrix with aspect ratios around $L/D = 25$.

Keywords: Thermotropic liquid crystalline copolyesters; PET blends; Fiber spinning

1. Introduction

Poly(ethylene terephthalate) (PET) fibers are employed in a variety of industrial applications such as tire cords, composites, belts, and textiles. The synthesis and fiber spinning procedures are well established and fiber properties can be optimized by the processing parameters, e.g. molecular weight, spinning speed, draw ratio and drawing temperature [1]. However, an improvement in fiber modulus around 30–40% without sacrificing tenacity accompanied by a minimal increase in manufacturing costs would be readily accepted by industry. In addition, the modified material should be processible with established melt spinning procedures, therefore not requiring changes in PET synthesis or spinning technologies. One concept of PET fiber reinforcement is the formation of in situ composites with thermotropic liquid crystalline polyesters (TLCP). In general, in situ composites are formed by the inclusion of TLCPs in an isotropic matrix. The reinforcing, fibrillated species is not present in the starting blend but is formed during processing [2]. For fibers in particular this is advantageous compared to solid fillers such as chopped glass fibers, since they cause wear on the processing equipment or increase the melt viscosity. In the past years many publications have dealt with the reinforcement of PET blends processed into extrudates and injection-molded parts, which will be not discussed here. However, the research activities in the field of the much more complicated fiber processing of PET/TLCP blends have been rather limited. Most spinning experiments were carried out on blends of PET and commercial TLCPs such as Vectra® [3–7] or PET/HBA, also marketed as Rodrun® LC [8–11]. Some disadvantages are the high transition temperatures and critical melt viscosities of the TLCP at typical PET melt processing temperatures. Fibrillation of the TLCP phase and an increase of the tensile modulus with load level and drawing speed are observed commonly for such undrawn systems. Two publications address the issue of drawability and improvements in the mechanical properties by a heat treatment of PET blend fibers [6,7]. Other research groups investigated ternary blend systems with polycarbonate as the third component [12,13] or the addition of a polyhydroxyether as a compatibilizer [14]. It was postulated that the compatibilizer enhances adhesion between PET and Vectra®. Another approach to improve adhesion between the PET matrix and TLCPs [15,16] is the application of semiflexible TLCPs first developed by Lenz and coworkers [17–20]. This concept is based on the idea that in carefully designed thermotropic block copolyesters,

* Corresponding author. Fax: +49-921-55-3670.
E-mail address: reiner.giesa@uni-bayreuth.de (R. Giesa).
[1] Present address: mnemoScience GmbH, 52074 Aachen, Germany.

0032-3861/01/$ - see front matter
PII: S0032-3861(01)00357-3

the flexible block provides better adhesion and compatibility to the matrix whereas the LCP block is responsible for mechanical load bearing in the final composite. In close collaboration with Lenz's group, Farris et al. investigated intensively the behavior and mechanical performance of blend fibers spun from PET and thermotropic block copolyesters featuring PET-similar segments [21–26]. Here the best results were observed with a so-called random copolyester [27] indicated by a 50% increase in modulus at 5 wt% load level while maintaining ultimate strength values [21,28].

Reviewing the results in PET/TLCP blend fibers, some requirements for the in situ reinforcement can be summarized.

(i) *Fibril formation*. The size, shape and distribution of the TLCP phase in the matrix polymer influences the mechanical properties of the blends. It is known that fiber in situ reinforcement requires the formation of TLCP fibrils in the PET matrix [11,29]. Fibril formation is essential for this concept, since spherical inclusions exert only a small influence on tensile properties whereas a fibrillar morphology induces an increase in mechanical performance. Fibril formation itself depends on several conditions which are briefly summarized here but is not intended to be complete: the *viscosity ratio* of TLCP and PET melt must be optimal. Results with other systems [30,31] indicate a ratio less than or equal to one is required for fibril formation. Increasing the processing temperature not only lowers the TLCP viscosity but also the viscosity of the PET matrix. Hence every blend system has an *optimal processing window* depending on the matrix polymer. For the PET grade used in this work this window is between 270 and 290°C. At lower temperatures the matrix viscosity is too high, at temperatures above 290°C increasingly transesterfication as one possible side reaction is observed. Although transesterfication has been deliberately caused in some cases [26,32], we intended clearly to avoid this reaction. The interfacial *adhesion* between the PET and TLCP phases is also critical [33]. Good adhesion determines the formation of droplets which can be extended to fibrils in an elongational shear field. Poor adhesion causes low shear friction between the matrix and TLCP thus impedes the formation of fibrils. On the contrary, too much adhesion suppresses fibril formation since both phases show no phase separation.

(ii) *Drawabilty*. Another important factor often neglected is the drawability of fibers spun from blends. PET requires extensive post-drawing to reach its maximum mechanical properties. After blending with TLCPs, in particular at loading-levels above 5 wt%, drawing is often impossible, with the material exhibiting embrittlement and fibers breakage at low elongations.

(iii) *Modulus of the reinforcing component*. According to the composite theory (vide infra), the modulus of the reinforcing fibrils must be sufficiently high to provide reinforcement effects even at lower loading levels. Although the neat mechanical properties of the above mentioned thermotropic block copolymers are not known or published, it is reasonable to assume that the flexible blocks decreases the modulus of the copolymer fibrils. Data for other semirigid LCP are available, for which moduli around 20 GPa at draw ratios of 200 have been determined [34].

This work now deals with a different TLCP as the in situ reinforcing component in PET fibers which has been not investigated before. For this purpose, fully aromatic liquid crystalline copolyesters were structurally modified with non-coplanar biphenyl units and a TLCP called CPHNA60 was chosen consequently for blending experiments [35]. This amorphous system only shows a glass transition around 100°C, no crystallization, and no isotropization up to 310°C, clearly above our PET processing window and hot-drawing temperature. In addition to blend characterization, the blend fiber morphology and mechanical performance as a function of TLCP load level is investigated.

2. Experimental

2.1. Materials

Fiber grade PET was received from Hoechst-Celanese Corp. in form of pellets with a solution viscosity of 0.73 dl/g at 80°C in 60:40 (wt/wt) phenol/1,1,2,2-tetrachloroethylene. This value corresponds to a molecular weight of 44,000 g/mol [36]. The liquid crystalline material employed in this study is a thermotropic copolyester with a structure shown in Scheme 1. Based on a content of 60 mol% 2-hydroxy-6-naphthoic acid (HNA) the copolyester will be referred to as CPHNA60. A detailed description of the synthesis, characterization, fiber spinning as well as other properties of this copolyester is published in the following article [35].

2.2. Blend preparation

To improve the mixing of PET and TLCP compared to the compression molding technique employed before [21,24], the blends in this work were prepared in a two-screw MiniMixer, developed at TU Eindhoven, Netherlands and now commercialized by DACA Instruments, USA [37]. Each mixing run was carried out at 280°C under dry nitrogen yielding batches of ca. 3 g, and at least three mixing runs were necessary for a typical spinning experiment requiring 9–12 g. The obtained 2 mm diameter rods were

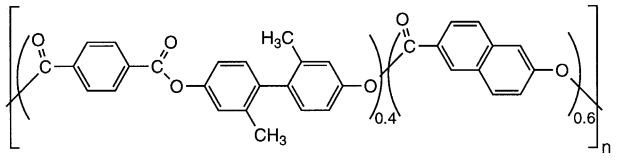

CPHNA 60

Scheme 1.

cut into pieces and ground at dry ice cooling in a Retsch Ultra Mill ZM 100 to a powder finer than 750 μm. This kind of powder is required for feeding the Randcastle 1/4-inch Microtruder. All materials were vacuum dried for at least 24 h at 90°C before mixing or spinning.

2.3. Extrusion and spinning

A Randcastle 1/4-inch Microtruder was used for the extrusion and spinning of the blends into fibers. This system consists of a barrel with a 0.25 in. extruder screw, a die block and the die (1575 μm bore diameter, 10:1 aspect ratio). The extruder has four heating zones, which can be controlled separately. For all experiments, heating zones one and two were set at 240 and 260°C, respectively, while the temperatures for zone three and the die block were always set identical and are listed explicitly in the text. Before and during spinning the feeding zone was flushed with dry nitrogen. The residence time was adjusted to 3–4 minutes by the extruder screw speed of 25–30 rpm. The fiber was drawn down for ca. 1 m and taken up at rates of 100 and 500 m/min on commercial fiber spools. The stretch down ratio of the as-spun fibers varied between 400 and 3000.

2.4. Post treatment

The as-spun fibers were immediately cold-drawn on a hot-plate at 90°C. Drawing of the fibers was performed in a continuous process between supply and take-up spools. The revolution speeds of the spools are electronically controlled and thus very constant. In addition the force developed in the fiber during drawing was recorded with a 2 N load cell. The speed of the take-up spool was continuously monitored and increased until the fiber neck remained constant at specific position above the hot-plate. For pure PET this was observed at speed ratios (SR) of 3.5–4, where the ratio is defined as $SR = v_{suppl}/v_{take\text{-}up}$. In the following hot-drawing step at 220°C the cold drawn fiber was drawn at a plate temperature of 220°C, with the maximum SR typically around 1.3. The draw ratio (DR) in this work is defined as the ratio of the square of the fiber diameters (D) before and after drawing, $DR = D^2_{undrawn}/D^2_{drawn}$, where the change in density is not considered in the definition. According to an internal testing procedure provided by Hoechst-Celanese, dimensional stability is optimal above the shrinkage test temperature of 177°C, thus 220°C was used as hot-drawing temperature.

2.5. Fiber testing

All fibers were tested according to ASTM Method D 3379 using a gauge length of 50 mm. Based on this standard the monofilaments were mounted on paper tabs which facilitates fiber handling. Prior to testing, the fiber diameters were determined with an Olympus BX60 optical microscope calibrated with a Leitz dimensional standard at a magnification of 500 for as-spun fibers and at 1000 for drawn fibers. The average of three measurements per fiber was used to calculate the cross sectional area of the monofilament. Tensile tests were carried out on an Instron Universal Tester (Floor Model 5565, 5 kN frame) with a 100 N Instron load cell and 100 N pneumatic grips with rubber jaw faces. For as-spun fibers a crosshead speed of 50 mm/min was chosen and hot-drawn fibers were tested at 5 mm/min. All reported mechanical data are an average of at least eight independent measurements, the standard deviation being given in the data tables.

Hot-drawn neat PET fibers with a modulus of 18.5 GPa and 7–8% elongation at break at an ultimate strength of 900–1000 MPa were used as a control for all experiments.

2.6. Scanning electron microscopy

The fiber morphology was investigated by scanning electron microscopy (SEM) in a Jeol JSM 840 A Scanning Microscope at 10 and 20 kV. The fibers were mounted on the sample holder, frozen in liquid nitrogen and fractured with tweezers yielding fracture surface in most cases below the tweezers grip. This method was found to result in cleaner fracture surfaces. The fiber pieces were sputtered with gold prior to scanning.

2.7. Other methods and instruments

Viscosity measurements were performed using a Schott–Ubbelohde viscosimeter in combination with a Lauda Visco Boy 2 control unit. Thermal transition temperatures were measured with a Perkin–Elmer DSC 7 Differential Scanning Calorimeter under nitrogen (40 ml/min) calibrated with indium. A Rheometric Scientific Stress Rheometer SR 5000 and 25 mm parallel plate geometry was used for all rheological measurements. This instrument was calibrated with Viscosity Standard 992 and 100 cp supplied by Rheometric Scientific.

3. Results and discussion

3.1. Blend preparation

The TLCP investigated in this study is a fully aromatic thermotropic copolyester (CPHNA60) with a structure shown in Scheme 1 and can be described as a copolymer of terephthalic acid, a non-coplanar twisted biphenyl moiety and HNA. By adding different amounts of HNA the copolyester properties have been tailored to the processing conditions required for spinning blends with PET. Here a composition of 60 mol% HNA was found to be optimal with regard to melt viscosity, with the fiber processing temperature matching the PET processing window and CPHNA60 fiber tenacity. This TLCP was characterized by an inherent viscosity of $\eta_{inh} = 2.05$ dl/g at 25 °C in TFA/$CHCl_3$ (1:1 v/v) and only a glass transition at 98°C. No other transitions were

Table 1
Transition temperatures and enthalpies obtained from DSC measurements for the CPHNA60/PET blends (heating and cooling rate: 10 K/min)

CPHNA60 [wt%]	T_g [°C]	T_{rc}[a] [°C]	ΔH_{rc} [J/g]	T_m [°C]	ΔH_m [J/g]	T_c[b] [°C]	ΔH_c [J/g]
0	81	164.6	−37.1	248.2	33.3	175.8	−35.6
0.5	81	138.0	−18.4	249.8	35.9	192.6	−39.3
1.5	81	131.4	−10.2	250.9	35.6	196.0	−41.2
3	82	131.1	−6.2	250.1	36.9	198.8	−42.6
5	80	139.8	−21.4	250.8	39.9	196.3	−44.3
10	81	137.1	−18.1	249.1	40.1	195.4	−47.0

[a] Recrystallization temperature from 2nd heating curve of quenched sample.
[b] Crystallization temperature from 2nd cooling cooling curve.

detected up to 310°C, so this material is considered a nematic glass at room temperature. The synthesis, characterization, spinning and fiber properties of CPHNA60 is published in the following article [35].

The blends were prepared under nitrogen in a miniature twin-screw mixer at 280°C for three minutes at 30 rpm. At a mixing volume of ca. 3 g three to four mixing runs were needed to obtain sufficient material for grinding and spinning. This mixing technique provides a more homogeneous blend preparation compared to a compression molding technique used in previous experiments [21,24]. Blends with load levels of 0.5, 1.5, 3, 5 and 10 wt% TLCP were prepared in this way.

3.2. Blend characterization

3.2.1. Differential scanning calorimetry

The influence of the added CPHNA60 on glass transition, melting and recrystallization temperatures of the blends was examined by differential scanning calorimetry (DSC). First the samples were quenched with a cooling rate of 500 K/min from 310 to 20°C, then the data listed in Table 1 were measured by a heating and cooling run at 10 K/min (Fig. 1).

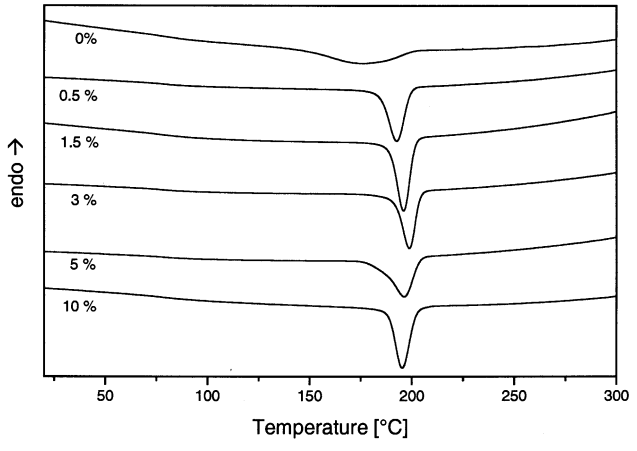

Fig. 1. DSC traces of 2nd cooling at 10 K/min for of PET/CPHNA60 blends. The samples were heated under nitrogen atmosphere to 350°C (1st heating), quenched to 20°C (1st cooling), and heated again with 10 K/min (2nd heating). All data are compiled in Table 1.

The melting and crystallization enthalpies are standardized regarding the PET content.

The DSC curves are similar to those obtained from pure PET, with a glass transition temperature (T_g) of 80°C and a melt endotherm around 250°C. The T_g of CPHNA60 is not detectable even at a content of 10 wt%. The melt temperatures of the blends are a few degrees above the reference value of neat PET, while the T_g differ by one degree only. In both cases, no dependency on the composition can be established. At cooling from the melt, the crystallization occurs sooner compared to PET, accompanied by a decrease in the width of the crystallization peak. Thus the crystallization occurs at higher temperature and proceeds faster than in PET. This effect is more pronounced at higher CPHNA60 load levels. The values for ΔH_c also indicate an increase in the degree crystallinity of the PET fraction. The added TLCP acts as nucleation agent in flexible thermoplastics, thus facilitating crystallization indicated by a higher recrystallization temperature and markedly faster crystallization process. This nucleating effect has been observed also in other systems [21,22,38–40]. The peak maximum is less broad and shifts to higher temperatures at only 0.5 wt% CPHNA60, with continuation of this trend up to 3 wt% TLCP. However, a further increase in TLCP concentration does not lead to improved nucleation. A similar behavior is observed for the recrystallisation peak during heating,

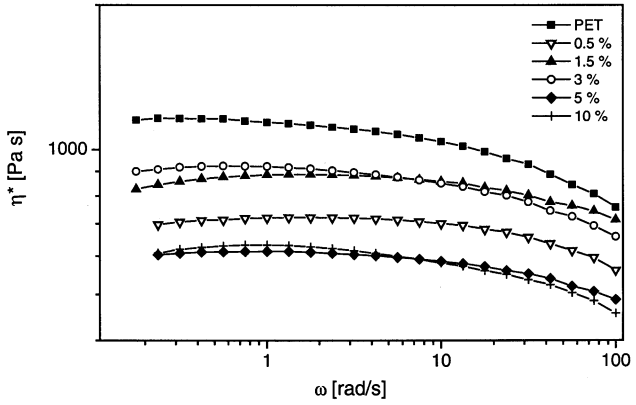

Fig. 2. Function of the complex viscosity η^* of blends at different load levels versus the shear rate determined in a parallel plate geometry at 280°C and a constant shear stress of 400 Pa.

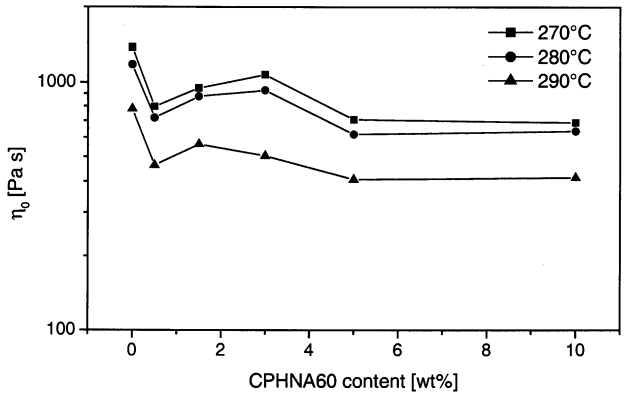

Fig. 3. Zero shear viscosity η_0 as a function of the blend composition at three different temperatures.

which decreases with 3 wt% up to 131°C, then rises again with higher concentrations. The corresponding ΔH_{rc} is also reduced at this concentration, which is the result of a high degree of crystallization during quenching.

3.2.2. Rheology

The complex viscosity of the PET/CPHNA60 blends was measured with a parallel plate geometry. The frequency response of η^* was determined within the linear viscoelastic region at a constant shear stress of 400 Pa (Fig. 2). The addition of CPHNA60 not only lowers the viscosity, but the frequency range is also extended over which the system possesses a zero shear plateau. In particular with 0.5, 5 and 10 wt% the curves are more linear compared to neat PET and Newtonian behavior is exhibited for shear rates up to 10 rad/s. A similar effect has been observed in blends of a semiflexible, segmented LCP and PET [41].

With the addition of CPHNA60 the melt viscosity of the system is reduced as shown in Fig. 2. At 10 wt% load level the viscosity is lowered to half of the value of neat PET. The zero-shear viscosity of the blends depends not monotonously on the concentration, at 0.5 wt% a strong decrease in η_0 is observed, then rises at 1.5 and 3 wt%, followed by a further decrease in η_0 with increasing load levels. This effect has been observed also in another blend system [42] and therefore apparently is not caused by a special effect of CPHNA60. The temperature dependence of the zero-shear viscosity (Fig. 3) is comparable to the PET reference over the entire concentration range. Increasing the temperature from 270 to 280°C causes a small decrease in viscosity only, while the viscosity is clearly reduced at 290°C.

The shear rates accessible in our measurements are small compared with those occurring during fiber spinning. At the shear and elongational flow fields at the end of the die, shear stresses and rates have a strong influence on the viscosity of the blend system. Investigations at high shear rates in a high-pressure capillary rheometer could not be performed due to insufficient amounts of CPHNA60 material. However, it is known from similar systems that shear thinning is very pronounced especially at higher shear rates [11,29,43–45].

3.3. Fiber processing and characterization

3.3.1. Blend fiber spinning

All blends up to 10 wt% CPHNA60 content could be spun into high quality monofilaments. A pronounced shear

Table 2
Tensile properties of as-spun blend fibers (E: modulus, σ_{br}: strength at break, ϵ_{br}: elongation at break, standard deviation in parentheses)

CPHNA60 [wt%]	v[a] [m/min]	T_{sp}[b] [°C]	D[c] [μm]	E [GPa]	σ_{br} [MPa]	ϵ_{br} [%]
0	100	280	54	2.27 (0.16)	106.0 (31.1)	288 (59)
0.5	100	280	80	2.26 (0.30)	83.6 (17.0)	371 (18)
1.5	100	280	82	2.68 (0.04)	81.3 (10.9)	407 (34)
3	100	280	65	3.06 (0.08)	80.3 (6.6)	421 (17)
3	100	290	46	2.13 (0.11)	21.9 (7.5)	206 (52)
5	100	270	55	3.74 (0.22)	97.9 (15.9)	389 (41)
5	100	280	66	3.37 (0.13)	82.5 (11.5)	435 (44)
10	100	270	52	5.80 (0.48)	94.2 (7.4)	2 (< 1)
10	100	290	43	5.57 (0.36)	84.9 (6.4)	7 (7)
0	300	280	32	2.30 (0.12)	124.2 (24.7)	250 (48)
0.5	300	280	39	2.40 (0.13)	172.5 (25.9)	292 (23)
1.5	300	280	42	2.69 (0.18)	150.8 (29.0)	360 (48)
3	300	280	33	3.03 (0.10)	117.7 (30.8)	298 (54)
3	300	290	41	2.38 (0.07)	45.3 (2.0)	293 (19)
5	300	270	32	3.82 (0.14)	59.0 (8.7)	246 (19)
5	300	280	36	3.73 (0.12)	72.0 (13.8)	298 (27)
10	300	270	31	6.44 (0.35)	105.3 (5.9)	3 (1)
10	300	290	30	5.64 (0.33)	89.6 (4.6)	2 (<1)
3	500	280	27	3.05 (0.59)	161.2 (31.1)	286 (25)

[a] Take-up (spinning) speed.
[b] Spinning (die) and zone three temperature.
[c] Fiber diameter determined by optical microscopy.

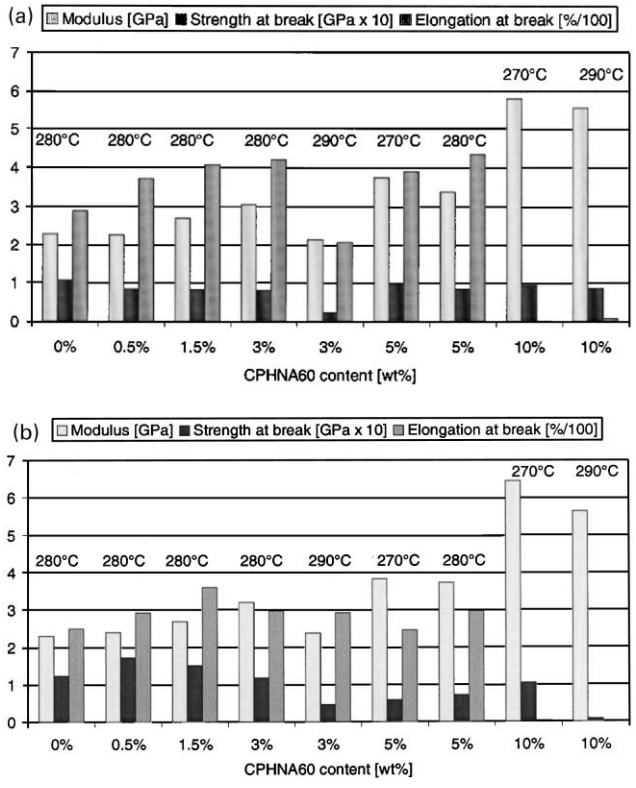

Fig. 4. (a) Tensile performance of as-spun blend fibers spun at 100 m/min as function of CPHNA60 content and spinning temperature. Numerical data are listed in Table 2. (b) Tensile performance of as-spun blend fibers spun at 300 m/min as function of CPHNA60 content and spinning temperature. Numerical data are listed in Table 2.

thinning effect was not observed. All blends were spun at 280°C and collected at 100 and 300 m/min. For select compositions, the spinning temperature was varied between 270 and 290°C. To study the influence of higher take-up rates the 3 wt% blend was additionally collected at 500 m/min. As-spun fibers were beige-opaque in color and homogeneous in appearance without the presence of any voids or included particles. Neat undrawn PET fibers, which were spun before hand as a control, are usually transparent or translucent.

3.3.2. Mechanical performance of as-spun blend fibers

Fibers were mounted on paper tabs, the diameters determined in a microscope and then Young's modulus, strength and elongation at break were measured in a tensile test. The results are summarized in Table 2; in Fig. 4a and b a presentation of mechanical data at 100 and 300 m/min are given, respectively. These bar diagrams illustrate clearly the numerical data of Table 2 and thus permit an easy comparison and recognition of trends within a series of tested fibers.

At take-up rates of 100 and 300 m/min the as-spun fibers show higher moduli with increasing CPHNA60 content. This increase suggests a reinforcement of the fibers by the TLCP component. The moduli are higher at higher take-up speeds, which can be attributed to an improved orientation of the TLCP domains in the fiber. However, the mechanical performance declines at higher spinning temperatures. This effect was observed before and explained by a decreased orientation in the PET fraction of the fiber [26]. The difference

Table 3
Tensile properties of post-treated (cold- and hot-drawn) blend fibers (E: modulus, σ_{br}: strength at break, ϵ_{br}: elongation at break, standard deviation in parentheses)

CPHNA60 [wt%]	v[a] [m/min]	T_{sp}[b] [°C]	D[c] [μm]	DR[d]	E [GPa]	σ_{br} [MPa]	ϵ_{br} [%]
0	100	280	22	6.17	18.90 (1.14)	1088.0 (58.2)	8.03 (0.75)
0.5	100	280	32	6.41	18.88 (0.78)	1148.1 (17.3)	8.53 (0.36)
1.5	100	280	31	6.83	20.40 (1.31)	1141.5 (48.4)	7.22 (0.80)
3	100	280	25	7.00	22.59 (1.32)	1171.6 (31.0)	6.58 (0.27)
5	100	270	25	4.75	18.86 (0.74)	930.7 (26.1)	7.23 (0.17)
5	100	280	22	9.19	22.10 (1.05)	1051.9 (46.4)	6.34 (0.30)
10	100	270	24	4.69	17.46 (1.06)	772.9 (47.0)	6.12 (0.59)
0	300	280	17	3.59	17.91 (1.41)	921.1 (49.0)	7.55 (0.76)
0.5	300	280	21	3.50	17.90 (1.24)	1153.5 (13.3)	7.41 (0.36)
1.5	300	280	20	4.21	17.97 (1.30)	1153.1 (13.0)	7.61 (0.27)
3	300	280	14	5.62	20.76 (1.66)	1153.9 (11.4)	6.68 (0.34)
5	300	270	16	4.01	18.04 (1.28)	824.8 (66.2)	6.83 (0.25)
5	300	280	17	4.72	18.81 (0.84)	899.9 (66.2)	6.81 (0.30)
10	300	270	15	4.35	17.49 (0.75)	726.1 (40.0)	7.33 (0.76)
3	500	280	13	4.41	18.02 (0.10)	1028.0 (62.6)	6.77 (0.66)

[a] Take-up (spinning) speed.
[b] Spinning (die) and zone three temperature for the as-spun fiber.
[c] Fiber diameter determined by optical microscopy.
[d] Draw ratio calculated by $D^2_{\text{as-spun}}/D^2_{\text{hot-drawn}}$.

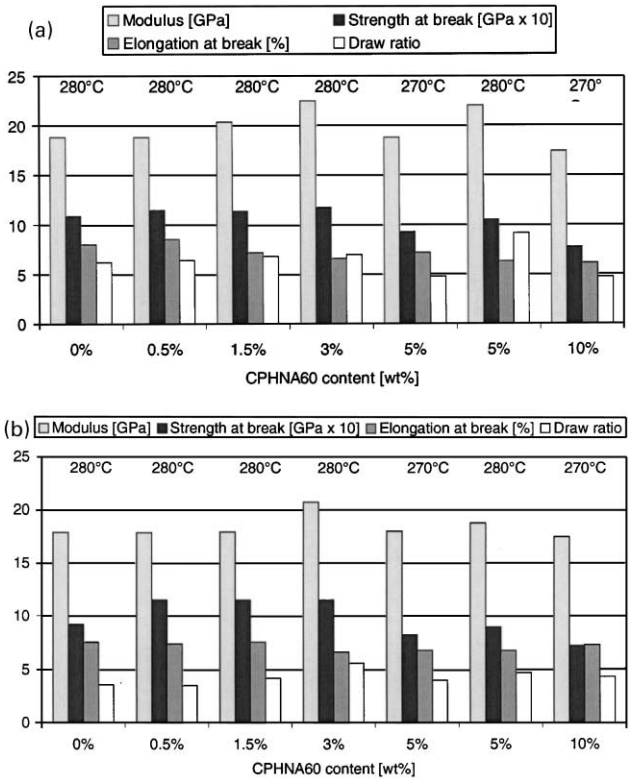

Fig. 5. (a) Tensile performance of post-treated blend fibers spun at 100 m/min as function of CPHNA60 content and spinning temperature. Fibers were first cold drawn at 90°C followed by hot-drawing at 220°C. Numerical data are listed in Table 3. (b) Tensile performance of post-treated blend fibers spun at 300 m/min as function of CPHNA60 content and spinning temperature. Fibers were first cold drawn at 90°C followed by hot-drawing at 220°C. Numerical data are listed in Table 3.

in performance between 270 and 280°C is smaller than that observed between 280 and 290°C. Simultaneously, a higher spinning temperature causes a smaller fiber diameter. The melt can be stretched more effectively since the melt viscosity clearly drops between 280 and 290°C, which is shown in Fig. 3. The tenacities of all fibers spun at 100 m/min are lower compared to the PET control. Hence, the TLCP phase negatively influences the orientation in the PET matrix. However, at 300 m/min the tenacities for low TLCP concentrations (i.e. 0.5, 1.5, and 3 wt%) are higher than the PET control but drop for load levels of 5 and 10 wt%. Extension at break increases for fibers up to 5 wt% content but drastically drops at 10 wt%. At this concentration the TLCP component is reinforcing the system but the elasticity of the matrix is lost and embrittlement occurs. This behavior is characteristic for TLCP strengthened, thermoplastic polymers [46], therefore higher load levels were not investigated. The increase in extension at break at low load levels is rather unusual for these systems but has been observed before [47]. A possible explanation for this observation might be that the TLCP functions as a tribological-active component between the PET chains, thus chain slippage is facilitated under load

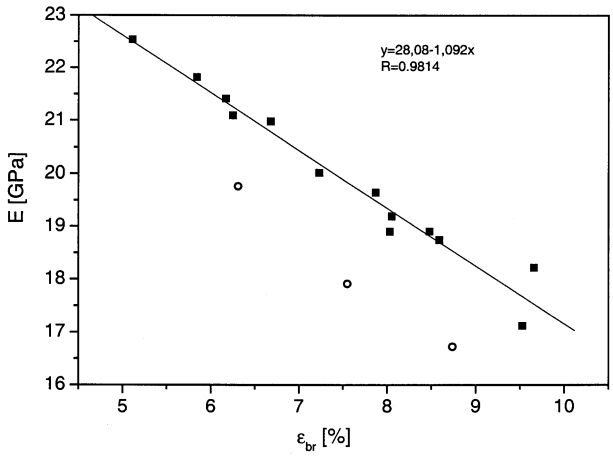

Fig. 6. Correlation of modulus and elongation at break for a variety of hot-drawn neat PET control fibers. Data represented by open circles were not included in the regression analysis. Fiber moduli up to 22.5 GPa can be attained by aggressive post-treatment conditions, however sacrificing elasticity.

and at the same time the reinforcing effect prevents fiber breakage.

3.3.3. Mechanical performance of post-treated blend fibers

All fibers were cold-drawn at 90°C as described in Section 2. The performance of the blend fibers during cold-drawing is similar to the PET control up to a CPHNA60 content of 5 wt%. At 10 wt% brittleness is critically increased and cold-drawing requires caution, however is still possible. All fibers spun at 290°C failed during cold-drawing and could not be post-treated. The performance of fibers during hot-drawing is more influenced by the quality of the cold-drawn fiber rather than the TLCP content. All monofilaments cold-drawn continuously at 90°C could be hot-drawn at temperatures up to 220°C without any problems. The drawing behavior is similar to the PET control for all compositions. All mechanical data of post-treated fibers are summarized in Table 3 and by Fig. 5a and b.

The moduli of the hot-drawn fibers are equivalent or slightly higher compared to the PET control. A clear trend in mechanical performance cannot be correlated to the composition. The tenacities at low load levels are somewhat higher than the PET control values, however at high load levels lower. Here again the draw ratio has a higher impact on tenacity than composition, whereby higher stretched fibers exhibit higher stresses at break. In the same way, the elongation at break is barely affected by the CPHNA60 content but is reduced at higher concentrations. Fibers spun at 270°C followed by hot-drawing exhibited poorer mechanical performance than fibers spun at 280°C. At 3 wt% TLCP load level an increase in the modulus to 22.6 GPa was achieved. This corresponds to an improvement of 22%. However, these moduli can be reached by extensive drawing, reflected by small elongations at break,

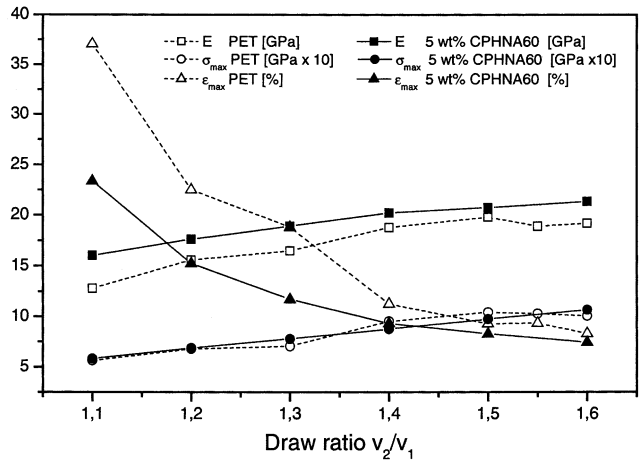

Fig. 7. Comparison of the mechanical performance of 5 wt% blend and PET control fibers cold-drawn at 90°C as function of the draw ratio during hot-drawing. Solid symbols: 5 wt% blend fiber, open symbols: PET control.

of the neat PET fiber alone. The plot shown in Fig. 6 was obtained after numerous drawing experiments with control fibers and illustrates the dependence of PET fiber modulus and elongation at break.

For optimal fiber performance, post-treatment of the fibers was optimized depending on their particular drawing behavior. However, in order to compare the mechanical data the drawing conditions for each individual fiber must be considered. To elucidate the influence of hot-drawing conditions on fiber performance, a 5 wt% TLCP blend fiber and a neat PET fiber were post-treated under the same conditions. The fibers were spun at 100 m/min, cold-drawn at 90°C and finally hot-drawn at 220°C at fixed draw ratios determined by the speed ratios of take-up and supply spool. A comparison between PET and blend fiber, which is illustrated in Fig. 7, reveals a higher modulus for the blend fiber compared to the PET control.

The tenacity shows the same trend with increasing draw ratio, in contrast to the modulus which shows only a weak dependence on the draw ratio. The elongation at break of both samples exhibits the typical reinforcing effect of the TLCP component. Hence, the blend fiber breaks at lower elongation than the PET control. With rising draw ratio both curves approach, since PET embrittles at higher draw ratios. A comparison between the drawing behavior of both systems reveals that the blend fiber is easier to draw beyond ratios of 1.5 and breaks less frequently than the PET fiber. For 5 wt% CPHNA60 an improvement in modulus is attained while maintaining the tenacity, however the reinforcing influence of the TLCP reduces fiber elasticity as well.

In an analogous experiment the influence of hot-drawing temperatures in the range of 150–220°C was tested [42] where it was shown that the hot-drawing temperature did not significantly influence the mechanical performance of PET or 5 wt% blend fiber. Varying the cold-drawing temperature to 70 or 100°C also neither changed the cold-drawing behavior nor affected the mechanical fiber properties attained after hot-drawing.

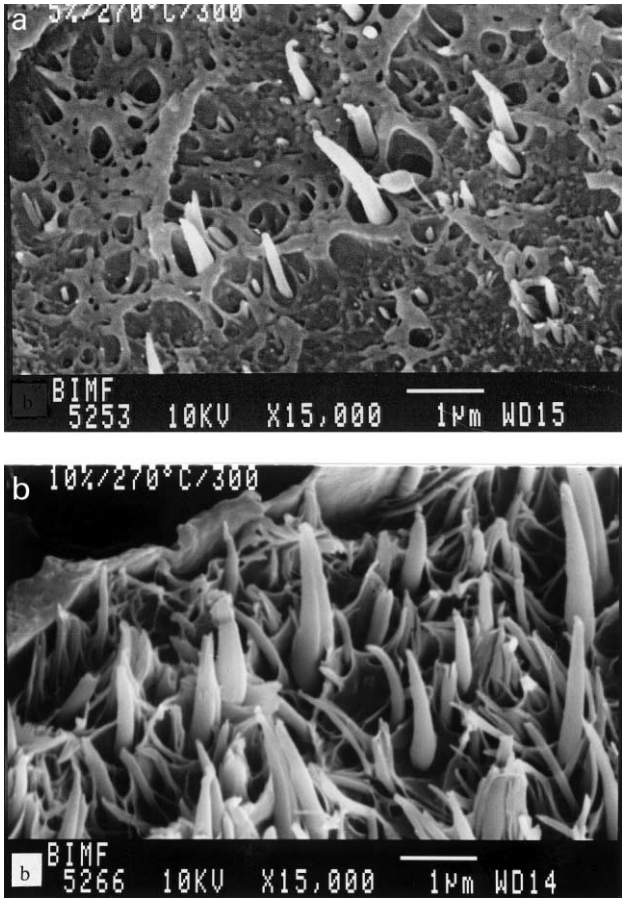

Fig. 8. SEM micrographs of as-spun blend fiber cross sections at 270°C at with 300 m/min. (a) 5 wt% CPHNA60; (b) 10 wt% CPHNA60.

3.3.4. Fiber morphology

Fracture surfaces were investigated by SEM perpendicular to the fiber axis. For as-spun samples, this technique revealed a distinct two-phase morphology with an oriented, fibrillar structure of the TLCP component embedded in the PET matrix. These fibrils were observed for all compositions between 0.5 and 10 wt% and there was no evidence of a critical concentration for fibrillation in the investigated range. Fig. 8a and b show detailed views of fracture surfaces of 5 and 10 wt% blend fibers, respectively.

The dimensions of the fibrils depend on the take-up speeds of the fibers, which is demonstrated in Fig. 9a and b. At a lower take-up speed of 300 m/min (Fig. 9a) the fibrils are thicker and longer, whereas at 500 m/min (Fig. 9b) many shorter and thinner fibrils are visible.

From a fibril diameter of approx. 200 nm and a length of 5 μm and longer, a minimum aspect ratio of $L/D = 25$ can be estimated. The length was determined from fracture surfaces parallel to the fiber axis and etching experiments [42]. There is no evidence for a core-shell morphology,

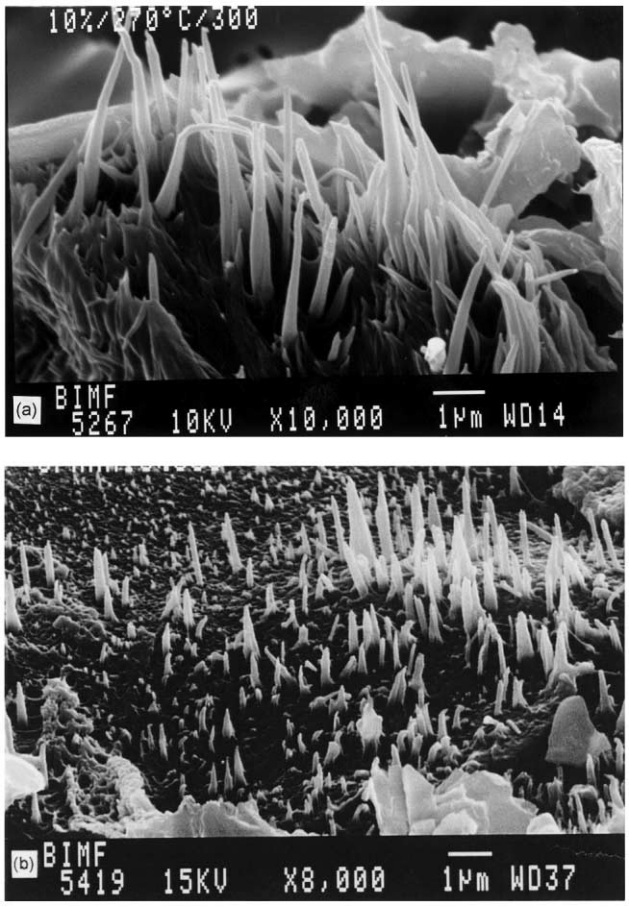

Fig. 9. SEM micrographs of as-spun blend fibers containing 10 wt% CPHAN60 spun at different speeds. (a) spun at 300 m/min; (b) spun at 500 m/min.

which is characterized by an inferior orientation in the core region of the fibers. In the investigated samples a concentration of thicker fibrils within the central regions of the fibers is not observed, on the contrary an even thickness distribution of the fibrils extends over the entire cross section. The adhesion of the TLCP fibrils at the PET matrix appears to be poor, since during the preparation of the fracture surfaces the fibrils are partly pulled out of the PET matrix and corresponding cavities are clearly visible. Furthermore, an opening is usually formed around the fibrils after fracture, which indicates a lack of adhesion between CPHNA60 and the matrix. However, the lack of adhesion might be an artifact of the sample preparation technique via cryo fracture caused by differences in thermal expansion of the components.

The formation of a fibrillar structure is essential for an improved mechanical performance of the blend fibers. The CPHNA60 chains should be oriented parallel within the fibrils and hence parallel to the fiber axis. The TLCP fibrils are consequently responsible for the improvement of the mechanical performance of the as-spun fibers, in particular for the modulus. The mechanical performance of the investigated blend fibers after hot-drawing, however, revealed

Fig. 10. SEM micrograph of a blend fiber containing 10 wt% CPHNA60 spun at 100 m/min and then cold drawn at 90°C.

only a modest increase, which is in contrast to the improvements found for as-spun fibers.

Several explanations are plausible for these results. It is possible that the fibrils are destroyed during hot-drawing. Since at 220°C the viscosity of CPHNA60 is low [35] destruction of the fibrils into very thin fragments under the tensile load applied during hot-drawing might be an explanation. This would cause a loss in the reinforcing effect of the TLCP phase. An additional possibility is lack of orientation of the TLCP within the fibrils. Then the fibrils would not achieve their optimal moduli and also the reinforcement would be weakened. Finally, the adhesion of the TLCP fibrils to the PET matrix might be critical. Poor adhesion between the two phases would cause an insufficient load transfer from the matrix to the fibrils.

To shed more light on possible failure mechanisms discussed above, the morphology of the drawn fibers was examined. As shown in Fig. 10 SEM investigations of the fracture surface of a cold-drawn fiber still indicates a fibrillar domain structure.

In the case of the hot-drawn fibers such SEM experiments were completely unsuccessful. The corresponding fiber cross section did not indicate any traces of a CPHNA60 phase. For instance, this could be caused by an insufficient contrast between the TLCP and the highly crystalline PET phase in the electron microscope, since both must be present in the fiber. Difficulties in the detection of the TLCP phase after hot-drawing however have been observed before with other PET/TLCP blend fibers [23]. Extensive etching experiments [42] were performed with hot-drawn blend fibers according to literature procedures [48] but still did not yield clearer information as to the kind of morphology of the CPHNA60 component in hot-drawn fibers.

3.3.5. Composite theory

The existence of fibrillar TLCP domains in as-spun PET/CPHNA60 blend fibers was detected in the morphology of the fracture surfaces. The Young's modulus of blend fibers

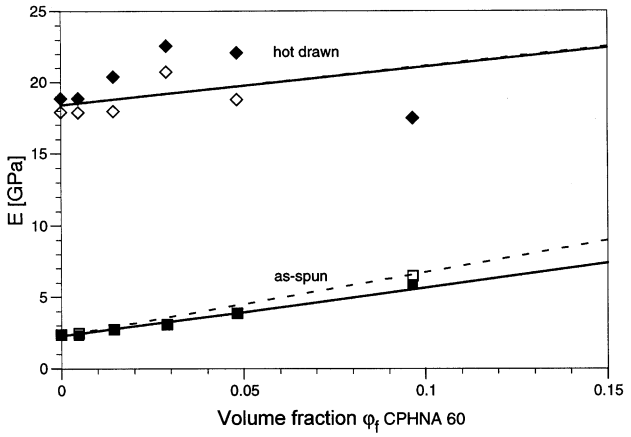

Fig. 11. Experimental blend fiber moduli compared to curves calculated by the rule of mixing (dashed line) and the Tsai–Halpin equation (solid line). Solid symbols: fiber spun at 100 m/min, open symbols: fiber spun at 300 m/min, squares: as-spun fibers, diamonds: hot-drawn fibers. (Data used for the Tsai–Halpin calculation: $E_f = 45$ GPa; $L/D = 25$; as-spun: $E_m = 2.3$ GPa; hot-drawn: $E_m = 18.4$ GPa).

can be estimated assuming the fibrils in the blend fiber possess the same mechanical characteristics of neat CPHNA60 fibers. Further assuming that the TLCP domains behave at room temperature similar to short glass fibers, the Tsai–Halpin equation (Eq. (1)) can be applied to calculate the blend fiber modulus [14,49–52].

$$\frac{E}{E_m} = \frac{1 + AB\varphi_f}{1 - B\varphi_f} \text{ with } A = \frac{2L}{D} \text{ and } B = \frac{E_f/E_m - 1}{E_f/E_m + A} \quad (1)$$

Here E is the modulus of the composite, E_m the modulus of the matrix, E_f and ϕ_f the modulus and the volume fraction of reinforcing phase, respectively, and L/D is the aspect ratio of the fibrils. As the aspect ratio approaches infinity, the fibrils can be approximated as continuous fibers and the Tsai–Halpin equation simplifies in the rule of mixtures, yielding Eq. (2).

$$E = (1 - \varphi_f)E_m + \varphi_f E_f \quad (2)$$

For the calculation, the modulus of the PET matrix was chosen as 2.3 GPa (see Table 2), for the CPHNA60 fiber a modulus of 45 GPa was determined [35], and for L/D a value of 25 was chosen as explained above. The weight fractions were converted to volume fractions with the densities of 1.332 g/cm^3 for as-spun PET and 1.386 g/cm^3 for CPHNA60. Fig. 11 depicts the experimental and calculated results according to Eqs. (1) and (2).

The experimental data for as-spun and hot-drawn blend fibers are compared to the curves obtained for the rule of mixture (dashed lines) and the Tsai–Halpin equation (solid lines). The values for as-spun fibers agree well with the Tsai–Halpin theory for low TLCP load levels. At 10 wt% the experimental value is higher, which could be explained by a larger axial ratio of longer fibrils than 25. A significant difference induced by the spinning rates is not reflected in the data. For the simple rule of mixture the measured moduli can be extrapolated by linear regression to a 100 wt% ($\varphi_f = 1$) composite or neat TLCP fiber. For fibers spun at 100 and 300 m/min, values of 37.9 and 43.4 GPa, respectively, are calculated for the moduli. These data are in reasonable agreement with the modulus of 45 GPa for a neat TLCP monofilament spun at a rate of 120 m/min [35].

For hot-drawn fibers the existence of TLCP fibrils could not be proven and therefore a determination of the axial ratio is not possible. For the calculation according to the Tsai–Halpin equation an axial ratio of the fibrils in the as-spun fibers ($L/D = 25$) was chosen. Moduli of 18.4 and 45 GPa were used for a drawn PET fiber and the CPHNA60 fibrils, respectively. As shown in Fig. 11 the Tsai–Halpin curve barely deviate from the simple rule of mixture, which reflects the upper limit for the infinite axial ratio. The experimental moduli of the fibers scatter around the theoretical curve. Particularly at low load levels the moduli are above both curves and a significant dependence on the spinning rate is present. Obviously effects occur, which cannot be described by the composite theory developed for fibrils similar to glass fibers. The reinforcing effect at low concentrations is stronger than that predicted by theory. At 10 wt% TLCP this effect is reversed and the moduli correspond more closely to neat PET without any reinforcement.

4. Conclusions

The objective of this work was the evaluation of a newly developed amorphous TLCP as an in situ reinforcement component in PET blend fibers. This liquid crystalline polyester, CPHNA60, shows only a glass transition far below and no isotropization at the PET processing temperature window and above. Therefore during spinning and drawing of the blends the TLCP remains in the nematic phase, which is expected to influence the overall mechanical behavior of the drawn blend fibers. Blend preparation, spinning into fibers and a two stage post-treatment in the form of cold and hot-drawing proceeded without any problems and load levels of 10% CPHNA60 were realized. A typical fibrillar microstructure of the TLCP for as-spun fibers was found in SEM investigations. The modulus of as-spun fibers increased with increasing CPHNA60 content in good agreement with the Tsai–Halpin theory. However, only a modest increase in modulus of about 22% to 22.6 GPa at 1200 MPa tenacity and a load level 3 wt% was determined for hot-drawn blend fibers. The best system published so far exhibits a modulus of 25 GPa at 5 wt% load level of a random copolymer [21,28]. For instance compared to data published by Bruggeman et al. [14], the modulus of our PET control fiber (18.5 GPa at a tenacity of 1000 GPa) is already clearly higher than their best reinforced blend system (16.7 GPa at a tenacity of 214 MPa). This shows that a comparison to the PET control is important and not the absolute mechanical properties. Although the reasons for the only modest

improvement with CPHNA60 remain speculatively at this moment, there exists the possibility, that just the broad nematic phase of this TLCP impedes a reinforcing effect after hot-drawing.

Acknowledgements

This work was partially funded by the Hoechst-Celanese Corporation (Summit, New Jersey). The authors are indebted to Dr O.R. Hughes for helpful suggestions and discussions. SEM investigations were performed with C. Drummer at the BIMF, which is gratefully acknowledged. We thank the Bavarian government for financial support under the program 'Neue Werkstoffe'.

References

[1] Hughes OR, Kurschus DK, Saw CK, Flint J, Bruno TP, Chen RT. J Appl Polym Sci 1999;74:2335.
[2] Kiss G. Polym Engng Sci 1987;27:410.
[3] Mithal AK, Tayebi A, Lin CH. Polym Engng Sci 1991;31:1533.
[4] Li JX, Silverstein MS, Hiltner A, Baer EJ. Appl Polym Sci 1992;44:1531.
[5] La Mantia FP, Cangialosi F, Pedretti U, Roggero A. Eur Polym J 1993;29:671.
[6] Liang B, Pan L, He X. J Appl Polym Sci 1997;66:217.
[7] Pan L, Liang B. J Appl Polym Sci 1998;70:1035.
[8] Mehta S, Deopura BL. Polym Engng Sci 1993;33:931.
[9] Mehta S, Deopura BL. J Appl Polym Sci 1995;56:169.
[10] Radhakrishnan J, Ito H, Kikutani T, Okui N. Polym Engng Sci 1999;39:89.
[11] Song CH, Isayev AI. J Polym Engng 1998;18:417.
[12] Kwon SK, Chung I. J Polym Engng Sci 1995;35:1137.
[13] Chapleau N, Carreau PJ, Peleteiro C, Lavoie PA, Malik TM. Polym Engng Sci 1992;32:1876.
[14] Bruggeman A, Tinnemans AHA. J Appl Polym Sci 1999;71:1107.
[15] Shin BY, Chung I. J Polym Engng Sci 1990;30:13.
[16] Shin BY, Jang SH, Chung IJ, Kim BS. Polym Engng Sci 1992;32:73.
[17] Antoun S, Lenz RW, Jin JI. J Polym Sci, Polym Chem Ed 1981;19:1901.
[18] Ignatious F, Lenz RW, Kantor SW. Macromolecules 1994;27:5248.
[19] Ignatious F, Lu C, Lenz RW, Kantor SW. Macromolecules 1994;27:7785.
[20] Ignatious F, Lu C, Kim J, Lenz RW, Kantor SW. J Polym Sci, Polym Chem Ed 1995;33:1329.
[21] Joslin SL, Giesa R, Farris RJ. Polymer 1994;35:4303.
[22] Joslin SL, Jackson W, Farris RJ. J Appl Polym Sci 1994;54:289.
[23] Joslin SL, Jackson W, Farris RJ. J Appl Polym Sci 1994;54:439.
[24] Giesa R, Joslin SL, Mélot D, Farris RJ. Polym Polym Compos 1995;3:333.
[25] Petrovic ZS, Farris RJ. J Appl Polym Sci 1995;58:1077.
[26] Petrovic ZS, Farris RJ. J Appl Polym Sci 1995;58:1349.
[27] Tendolkar A, Narayan-Sarathy S, Kantor SW, Lenz RW. Polymer 1995;36:2463.
[28] Farris RJ, Joslin SL, Giesa R. US patent, 5,232,778, 1993.
[29] Song CH, Isayev AI. Polymer 2001;42:2611.
[30] Beery D, Kenig S, Siegmann A. Polym Engng Sci 1991;31:451.
[31] Siegmann A, Dagan A, Kenig S. Polymer 1985;26:1325.
[32] Magagnini P, Tonti MS, Masseti M, Paci M, Minkova LI, Miteva TT. Polym Engng Sci 1998;38:1572.
[33] Qiao F, Milger KB, Hunston DL, Han CC. Polym Engng Sci 2001;41:77.
[34] La Mantia FP, Valenza A, Citta V, Pedretti U, Roggero A. J Polym Sci B: Polym Phys 1993;31:933.
[35] Grasser W, Schmidt H-W, Giesa R. Polymer, 2001;42:8529.
[36] Brandrup J, Immergut EH, editors. Polymer handbook. 3rd ed. New York: Wiley, 1989. p. V/105.
[37] Maric M, Macosko CW. Polym Engng Sci 2001;41:118.
[38] Hong SM, Hwang SS, Seo Y, Chung IJ, Kim KU. Polym Engng Sci 1997;37:646.
[39] Kim SH, Park SW, Gil ES. J Appl Polym Sci 1998;67:1383.
[40] Ou CF, Huang SL. J Appl Polym Sci 2000;76:587.
[41] Lin YG, Lee HW, Winter HH, Dashevsky S, Kim KS. Polymer 1993;34:4703.
[42] Grasser W. PhD dissertation, University of Bayreuth, 1999.
[43] Kohli A, Chung N, Weiss RA. Polym Engng Sci 1989;29:573.
[44] Blizard KG, Baird DG. Polym Engng Sci 1987;27:653.
[45] Hong S, Kim B, Hwang S, Kim K. Polym Engng Sci 1993;33:630.
[46] Kulichikhin VG, Platé NA. Polym Sci USSR 1991;33:1.
[47] Mehta A, Isayev AI. Polym Engng Sci 1991;31:971.
[48] Zeronian SH, Inglesby MK, Pan N, Lin D, Sun G, Soni B, Alger KW, Gibbon JD. J Appl Polym Sci 1999;71:1163 and references cited therein.
[49] Halpin JC, Kardos JL. Polym Engng Sci 1976;16:344.
[50] Chen J, Harrison IR. Polym Engng Sci 1998;38:371.
[51] Kyotani M, Kaito A, Nakayama K. Polymer 1992;33:4756.
[52] Dutta D, Weiss RW, Kristal K. Polym Engng Sci 1993;33:838.